[Regular Paper]

Adsorption of Carbon Dioxide on Aminosilane-modified Mesoporous Silica

Norihito Hɪʏᴏsʜɪ, Katsunori Yᴏɢᴏ*, and Tatsuaki Yᴀsʜɪᴍᴀ

Research Institute of Innovative Technology for the Earth, 9-2 Kizugawadai, Kizu-cho Sorakugun, Kyoto 619-0292, JAPAN

Aminosilane-modified mesoporous silica was prepared by grafting various aminosilanes on mesoporous silica, SBA-15, and the applicability as a novel adsorbent for CO_2 capture and separation from flue gases was examined. Pore walls of SBA-15 were modified uniformly with aminosilanes by grafting and relatively high surface area and uniform pore size were retained. Adsorption capacities of CO_2 in the presence of water were compared with those in the absence of water by a flow method. Adsorption capacities of aminosilane-modified SBA-15 were comparable in the presence and absence of water vapor. In particular, the adsorption capacity of (3-trimethoxysilylpropyl)diethylenetriamine SBA-15 reached 1.2 mmol·g^{-1} in the presence of water vapor at 333 K, which is comparable to the adsorption capacity of zeolite Na-Y in the absence of water vapor. In addition, these adsorbents were completely regenerated by heating to 423 K in a He flow.

1. Introduction

The gradual increase in the atmospheric concentration of CO_2 due to fossil fuel combustion is becoming a serious environmental problem. Recently, CO_2 capture and sequestration have attracted considerable attention as one of the options to reduce CO_2 emissions. Various processes, such as liquid solvent absorption[1], membrane separation[2], and pressure (and/or temperature) swing adsorption (P(T)SA)[1,3] have been proposed for the separation and recovery of CO_2 emitted by power plants[1]. However, the costs of CO_2 separation from flue gases account for approximately 70-80% of the total energy cost for CO_2 sequestration. Therefore, it is important to develop new efficient and energy-efficient techniques for CO_2 separation. In addition, smaller plants are desirable for CO_2 separation, because enormous amounts of gases must be treated.

The conventional PSA or PTSA process using zeolite requires a dehumidification process which consumes about 30% of the total energy, because water vapor is adsorbed more strongly than CO_2 on a zeolite surface. Therefore, a new adsorbent which preferably adsorbs CO_2 in the presence of water vapor is required to develop a simple and energy-efficient process by elimination of the dehumidification process. Hydrated potassium carbonate supported on active carbon can absorb CO_2 from gas containing water vapor[4]. Solid sorbents in which amines are supported on high surface area supports are also promising as sorbents for CO_2 separation[5,6]. For example, aminosilane-modified silica gel has been applied as a CO_2 adsorbent[6].

Aminosilane-modified silica has been extensively studied because of the wide range of applications[7]. However, it is difficult to modify the micropore walls of silica with aminosilane molecules due to steric hindrance[7]. Therefore, mesoporous silicas such as M41S, FSM-16, and SBA-15 are regarded as more suitable supports for surface modification with aminosilane, because they have large and uniform pores. Furthermore, higher loading of aminosilane than in conventional silica gel should be possible due to the high surface area of mesoporous silicas. Aminosilane-modified mesoporous silica has excellent properties for the adsorption of heavy metals[8] and proteins[9], and for base-catalyzed reactions[10]. However, the adsorption of carbon dioxide on SBA-15 modified with (3-aminopropyl)triethoxysilane is not adequate[11]. Polyethylenimine-modified MCM-41 is an efficient CO_2 adsorbent[12,13], but the effect of water vapor on the adsorption characteristics of this material remains unknown.

SBA-15 is a suitable mesoporous silica for applications in gases containing water vapor due to its higher hydrothermal stability[14]. In this study, aminosilane-modified mesoporous molecular sieve SBA-15 was prepared as a "water-tolerant adsorbent" to adsorb CO_2

---

  * To whom correspondence should be addressed.
  * E-mail: yogo@rite.or.jp

in the presence of water vapor, and the applicability for PTSA was examined by CO_2 adsorption-desorption measurement in a flow system.

2. Experimental

2. 1. Preparation of Adsorbents

SBA-15 was prepared by a similar method to that reported by Zhao *et al.*[14]. Tetraethoxyorthosilicate (TEOS) was added to an aqueous solution of *block*-polyethyleneglycol-*block*-polypropyleneglycol-*block*-polyethyleneglycol with M_n of 5800 ($EO_{20}PO_{70}EO_{20}$, Aldrich) as a structure directing agent. After stirring for 5 min, 36% hydrochloric acid (Wako Pure Chem. Ind., Ltd.) was slowly added to the solution. The composition of the reaction mixture was TEOS 0.53 mol: $EO_{20}PO_{70}EO_{20}$ 50 g: HCl 2.0 mol: H_2O 80 mol. The mixture was heated with stirring at 303 K for 20 h, and then at 368 K for 24 h. The precipitate was filtered and washed with 4000 cm^3 of distilled water, then dried at 343 K over night. To remove the structure directing agent, the dried precipitate was calcined in air at 823 K for 8 h. The 2-D hexagonal structure characteristic of SBA-15 was confirmed by X-ray diffraction (XRD). The lattice constant of SBA-15 was estimated to be 11.3 nm by XRD.

Modification of SBA-15 was performed by the grafting method using aminosilanes. (3-Aminopropyl)triethoxysilane (APS, Aldrich), *N*-(2-aminoethyl)-3-aminopropyltriethoxysilane (AEAPS, Chisso Corp.) and (3-trimethoxysilylpropyl)diethylenetriamine (TA, Gelest Inc.) were used as grafting agents. Aminosilane (50 cm^3) and SBA-15 (5.0 g), which was previously dried at 398 K for 6 h in air, were refluxed in dehydrated toluene (250 cm^3) (Wako Pure Chem. Ind., Ltd.) at 383 K for 24 h under Ar flow. The product was washed once with toluene (200 cm^3) and dried at 333 K overnight. The obtained samples were named APS/SBA, AEAPS/SBA and TA/SBA.

Another sample named APS/SBA(i) was prepared by an impregnation method. APS (16.5 g) was impregnated into SBA-15 (5.0 g). The resultant mixture was heated at 333 K under saturated water vapor for 24 h, and then dried in air at 373 K for 24 h.

A gelatinous solid named APG was obtained by hydrolysis and condensation of APS. APS was heated at 333 K under saturated water vapor, and then dried at 373 K for 24 h. This treatment involved the following reaction (Eq. (1)).

$$NH_2(CH_2)_3Si(OCH_2CH_3)_3 + 1.5H_2O$$
$$\longrightarrow NH_2(CH_2)_3SiO_{1.5} + 3CH_3CH_2OH \qquad (1)$$
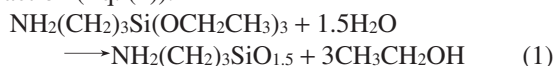
To determine the density of APG, the weight of a mixture of toluene and 2 g of APG (total volume: 10 cm^3) and the weight of 10 cm^3 of toluene was measured, and then the density of APG was calculated from these values.

2. 2. Characterization of Adsorbents

N_2 adsorption-desorption isotherms were measured at 77 K by a N_2 adsorption system (Autosorb 1, Quantachrome Co.) after each sample was stood in a vacuum at 473 K for 3 h. The surface areas and the pore size distributions were calculated by the BET and BJH method, respectively.

TG-DTA (thermogravimetry differential thermal analysis) curves of aminosilane-modified SBA-15 and APG were obtained with a thermal analysis system (TAS2000, Rigaku Corp.). The sample (*ca.* 10 mg) was heated in air at 5 $K \cdot min^{-1}$.

2. 3. CO_2 Adsorption-desorption Experiment

The capacity for CO_2 adsorption was determined by a flow method as follows. The adsorbent (1.5 g) was placed in a Pyrex tube (13 mm in inner diameter) and dried in a He flow (30 $cm^3 \cdot min^{-1}$) at 423 K for 1 h. A mixture of 12% H_2O with He balance (total flow rate: 60 $cm^3 \cdot min^{-1}$) was fed to the adsorbent at 333 K until the adsorbent was saturated with water, and then the gas flow was switched to a mixture of 15% CO_2, 12% H_2O with N_2 balance (total flow rate: 30 $cm^3 \cdot min^{-1}$). The breakthrough curve of CO_2 was obtained by the analysis of effluent gases. The effluent gases were analyzed with a gas chromatograph (GC-332, GL Science Inc.) equipped with a gaskuropack 54 column (2 m) and a thermal conductivity detector. Measurement of CO_2 adsorption-desorption capacity under dry conditions was conducted as follows: a mixture of 15% CO_2 with N_2 balance (total flow rate: 30 $cm^3 \cdot min^{-1}$) was fed to the dried adsorbent at 333 K without preadsorption of water vapor. The desorption experiment after CO_2 adsorption described as above was performed by heating from 333 to 423 K in a He flow (total flow rate: 30 $cm^3 \cdot min^{-1}$) at 10 $K \cdot min^{-1}$. Desorption curves were obtained by the analysis of effluent gases.

2. 4. Infrared Spectroscopy

Infrared spectra were obtained with a fourier transform infrared spectrometer (FT/IR-610, Jasco Co.) equipped with an MCT (mercury cadmium teluride) detector. Spectra were recorded at a resolution of 4 cm^{-1} with 64 scans. An APS/SBA pellet (20 mg, 20 mm in diameter) placed in a flow cell with ZnSe windows was heated in a He flow at 423 K for 1 h. A mixture of 2.3% H_2O with He balance was fed to the cell at 333 K for 30 min, and then the gas introduced was switched to the mixture of 3% CO_2 and 2.3% H_2O with He balance. A difference spectrum was obtained by subtracting the spectrum before CO_2 adsorption from that after CO_2 adsorption. In the case of measurement under dry condition, a mixture of 3% CO_2 with He balance was fed into the cell without preadsorption of water vapor.

3. Results and Discussion

3. 1. Characterization of the Adsorbents

Figure 1 shows the TG curves of calcined SBA-15, APG and APS/SBA. The TG curve of SBA-15 showed that weight loss continued only up to 390 K due to desorption of physisorbed water. The TG curve of APG showed two-stage weight loss: the first endothermic step with weight loss of 9.6% up to 390 K was due to desorption of physisorbed water, and the second exothermic step with weight loss of 40.7% between 500 and 920 K was due to combustion of organic moieties. The weight loss at the second step was 45.0% of the "dry base," and close to the value (45.5%) expected from Eq. (2), where $NH_2(CH_2)_3SiO_{1.5}$ is the composition of APG, as expected from Eq. (1).

$$NH_2(CH_2)_3SiO_{1.5} + xO_2$$
$$\longrightarrow SiO_2 + \text{combustion products} \uparrow \qquad (2)$$
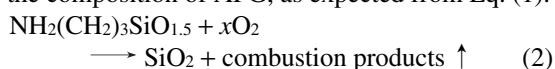
The TG curve of APS/SBA was similar to that of APG, with weight losses due to desorption of water and due to combustion of organic moieties from 470 K. Therefore, APS/SBA can be used in air at less than 423 K, at which APS/SBA is completely regenerated. This observation is similar to the cases of AEAPA/SBA and TA/SBA.
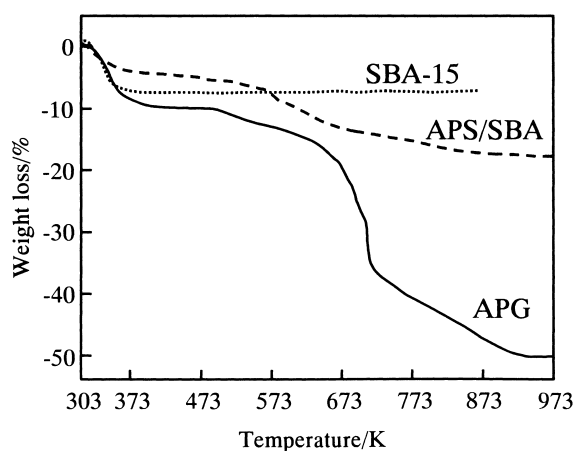

Fig. 1 TG Curves of SBA-15 (dotted line), APS/SBA (broken line) and APG (solid line) in Air

The compositions, numbers of aminosilane molecules per 1 nm^2 of SBA-15 surface area, and amine contents are summarized in **Table 1**. These values were determined from the TG weight losses due to combustion of organic moieties. The numbers of aminosilanes anchored to SBA-15 decreased in the order: APS/SBA > AEAPS/SBA > TA/SBA. This order is reasonable if the molecular sizes of aminosilanes are considered. On the other hand, the amine content increased in the order: APS/SBA < AEAPS/SBA < TA/SBA.

Surface coverage was calculated on the basis of the cross section area of anchored aminosilane at monolayer coverage (a_m) estimated by Eq. (3)[15],

$$a_m = 1.091 \cdot (M/N \cdot d)^{2/3} \qquad (3)$$

where N denotes the Avogadro number. M and d are the molecular weight and density of aminosilane gel obtained by hydrolysis and condensation of aminosilane, respectively. In Eq. (3), anchored aminosilane molecules are assumed to be spherical and form close-packed structures. The surface coverage of aminosilane was estimated to be 79, 78 and 92% for APS/SBA, AEAPS/SBA and TA/SBA, respectively. Therefore, the coverage of aminosilane anchored by the grafting method was estimated to be less than a monolayer.

The surface areas of the adsorbents were measured by N$_2$ adsorption at 77 K. **Figure 2** shows the N$_2$ adsorption-desorption isotherms of SBA-15 and aminosilane-modified SBA-15 at 77 K. The isotherms of APS/SBA, AEAPS/SBA and TA/SBA were classified as type IV, like that of SBA-15, indicating that the original mesoporous structure was still retained for these adsorbents. Although modification of SBA-15 with aminosilanes reduced the amounts of adsorbed N$_2$, higher surface areas were retained for APS/SBA, AEAPS/SBA and TA/SBA (**Table 1**). On the other hand, the surface areas of APS/SBA(i) and APG were very low (2 m$^2 \cdot$g^{-1}).

Figure 3 shows the pore size distributions obtained from desorption branches of the isotherms of SBA-15 and aminosilane-modified SBA-15. The mean pore diameters of APS/SBA, AEAPS/SBA and TA/SBA were smaller than that of SBA-15 (6.0 nm), indicating

Table 1 Physical and Chemical Properties of Adsorbents

Adsorbent	$SA^{a)}$ [m$^2 \cdot$g^{-1}]	Composition$^{b)}$	$N^{c)}$ [molecule$\cdot$nm^{-2}]	Amine contents$^{d)}$ [N-mmol$\cdot$g^{-1}]
SBA-15	910	SiO_2	0	0
APS/SBA	360	$SiO_2 \cdot 0.24(C_3H_8NSiO_{1.5})$	2.6	2.7
AEAPS/SBA	310	$SiO_2 \cdot 0.18(C_5H_{13}N_2SiO_{1.5})$	2.0	4.2
TA/SBA	240	$SiO_2 \cdot 0.16(C_7H_{18}N_3SiO_{1.5})$	1.8	5.1
APA/SBA(i)	2	$SiO_2 \cdot 1.10(C_3H_8NSiO_{1.5})$	12	6.0
APG	2	$C_3H_8NSiO_{1.5}$	—	9.0

a) Surface area calculated by BET method. b) Estimated by TG analysis. c) Number of organosilane molecules adhering per 1 nm^2 of SBA-15 surface. d) Defined as the number of nitrogen atom per 1 g of the adsorbent.
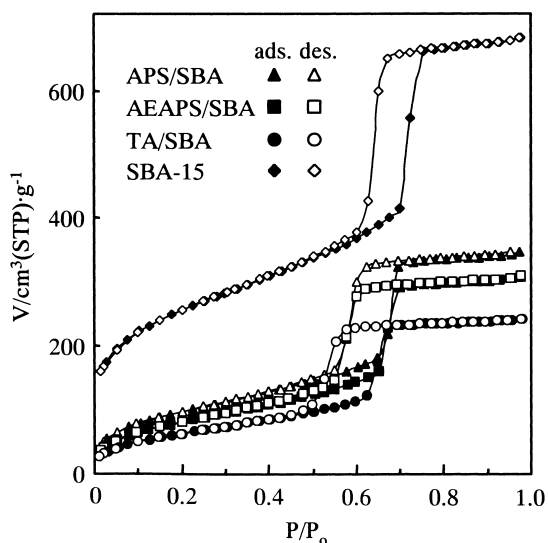
The solid and open points indicate measurements during adsorption and desorption processes, respectively.

Fig. 2 N_2 Adsorption-desorption Isotherms of APS/SBA (▲, △), AEAPS/SBA (■, □), TA/SBA (●, ○) and SBA-15 (◆, ◇) at 77 K
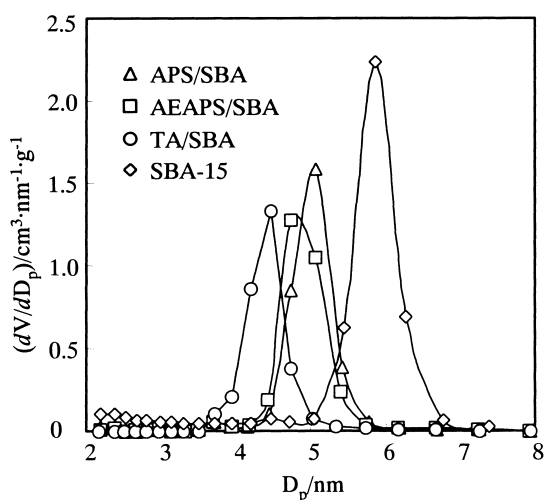

Fig. 3 Pore Size Distributions of APS/SBA (△), AEAPS/SBA (□), TA/SBA (○) and SBA-15 (◇) Calculated from the Desorption Branch by the BJH Method

homogeneous fixation of aminosilane molecules on the pore wall of SBA-15. Longer organic chains of aminosilane were associated with smaller pore size of aminosilane-modified SBA-15. In particular, the mean pore diameter was decreased to 4.8 nm by modification with TA. However, the sharp pore size distribution of SBA-15 was maintained after modification with aminosilanes by grafting. This suggests that the pore wall of SBA-15 was uniformly modified with amines by grafting.
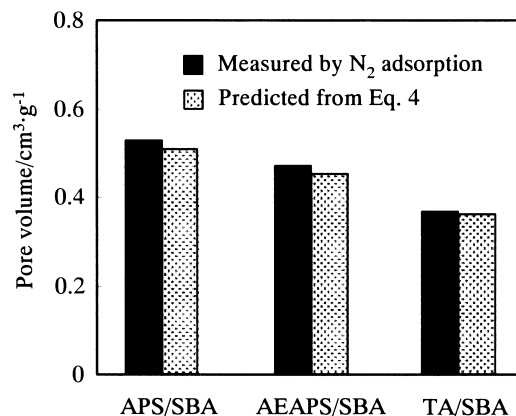

Fig. 4 Comparison of Pore Volumes Measured by N_2 Adsorption with Those Predicted from Eq. (4)

Figure 4 compares the pore volumes measured by N_2 adsorption with the predicted value (V_{cal}; $cm^3 \cdot g^{-1}$) from Eq. (4). In Eq. (4), V_{SBA} and w are pore volume of SBA-15 ($cm^3 \cdot g^{-1}$) and aminosilane loading (wt%) determined by TG analysis, respectively, and d is the density ($g \cdot cm^{-3}$) of corresponding aminosilane gel obtained by hydrolysis and condensation of aminosilane.

$$V_{cal} = V_{SBA} \times (100 - w)/100 - w/(100 \times d) \qquad (4)$$

The measured pore volume was very close to the predicted value for each adsorbent. This result indicates that SBA-15 was modified without pore plugging.

3. 2. Adsorption-desorption Properties

The breakthrough curves of CO_2 in the presence and absence of water vapor are compared in **Fig. 5**, and the CO_2 adsorption capacities obtained from the breakthrough curves are summarized in **Table 2**. In the breakthrough curves over only SBA-15, the relative concentration of CO_2 immediately reached unity due to the low adsorption capacity. On the other hand, considerable amounts of CO_2 were adsorbed on APS/SBA, AEAPS/SBA and TA/SBA. These aminosilane-modified SBA-15 had almost the same adsorption capacity in the presence and absence of water vapor. In particular, the adsorption capacity of TA/SBA reached 1.2 $mmol \cdot g^{-1}$ in the presence of water vapor. These results demonstrate that aminosilane-modified SBA-15 is effective for CO_2 adsorption under both dry and moist conditions.

Amine efficiencies of APS/SBA, AEAPS/SBA and TA/SBA, as defined by Eq. (5), are summarized in **Table 2**.

Amine efficiency
$$= adsorbed CO_2/amine content \qquad (5)$$

The amine efficiencies of these adsorbents were similar, as adsorption capacity is proportional to the amine content of the adsorbents. Therefore, primary amine and secondary amine are involved in CO_2 adsorption with similar efficiency.
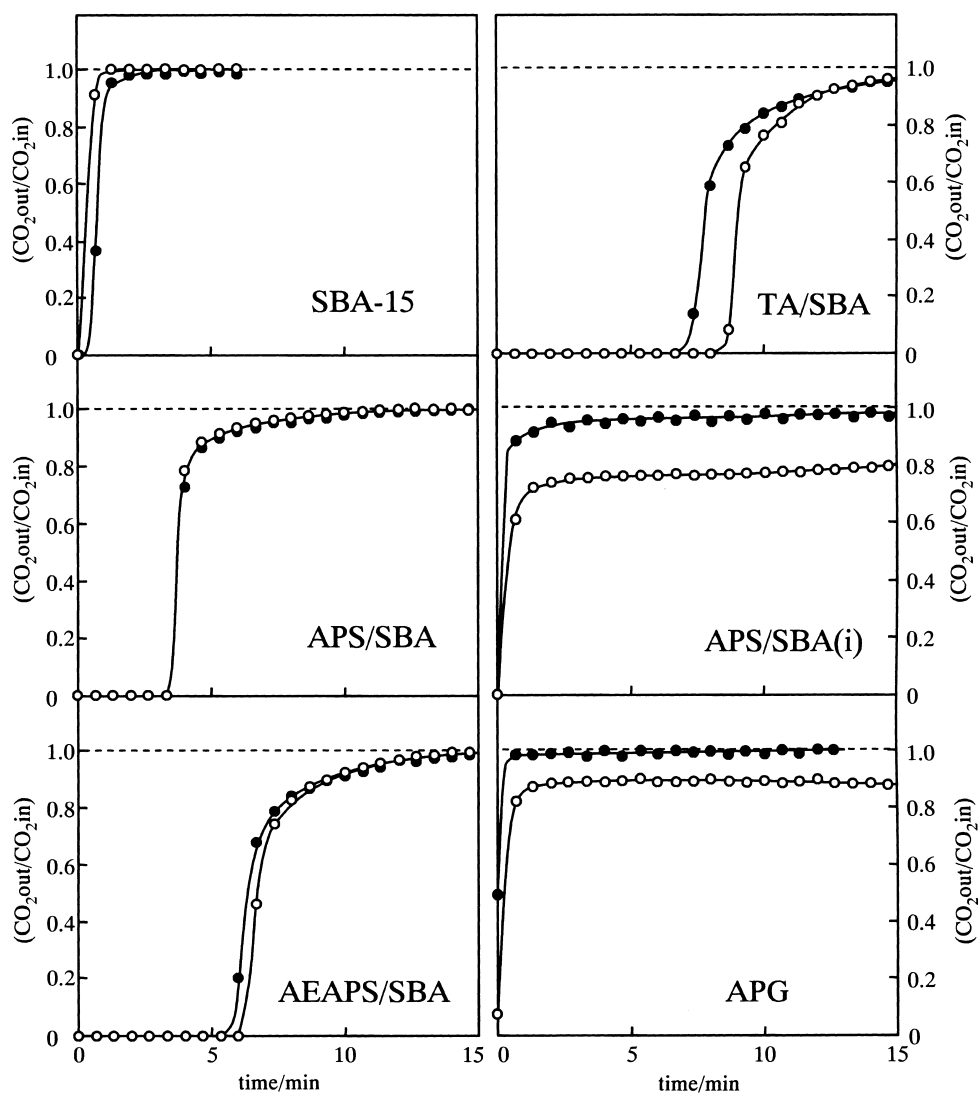
Adsorbent weight: 1.5 g, total flow rate: 30 cm³·min⁻¹.

Fig. 5 Breakthrough Curves of CO_2 Measured at 333 K with 15% CO_2 with N_2 Balance (●), and 15% CO_2, 12% H_2O with N_2 Balance (○)

Table 2 Capacities of Various Adsorbents for CO_2 Adsorption at 333 K

Adsorbent	Adsorbed CO_2 [mmol·g⁻¹ (amine efficiency[a])]	
	0% H_2O[b]	12% H_2O[c]
SBA-15	0.05	0.04
APS/SBA	0.52 (0.19)	0.50 (0.19)
AEAPS/SBA	0.87 (0.21)	0.90 (0.21)
TA/SBA	1.10 (0.22)	1.21 (0.24)
APS/SBA(i)	0.14 (0.01)	2.32 (0.39)
APG	0.03 (0.00)	2.71 (0.30)
Na-Y[d]	1.23	0.03

a) Amine efficiency = adsorbed CO_2/amine content. b) 15% CO_2 with N_2 balance. c) 15% of CO_2, 12% H_2O with N_2 balance. d) Si/Al = 2.7

The adsorption properties of zeolite Na-Y, APS/SBA(i) and APG were very different from aminosilane-modified SBA-15. Adsorption of CO_2 did not occur on zeolite Na-Y (Si/Al = 2.7) in the presence of water vapor. Adsorption of CO_2 was observed only in the presence of water vapor on APS/SBA(i) and APG. In spite of the low surface area, the CO_2 adsorption capacities of APS/SBA(i) and APG were much higher than that of aminosilane-modified SBA-15 in the presence of water vapor. The amine-CO_2 reaction on APS/SBA(i) and APG is associated with swelling with water or hydrolysis of siloxane bonds, which would enable the interior amino groups of the solid to react with CO_2. However, the breakthrough curves show that the rate of CO_2 adsorption on APS/SBA(i) and APG is much lower than on APS/SBA, AEAPS/SBA and TA/SBA.
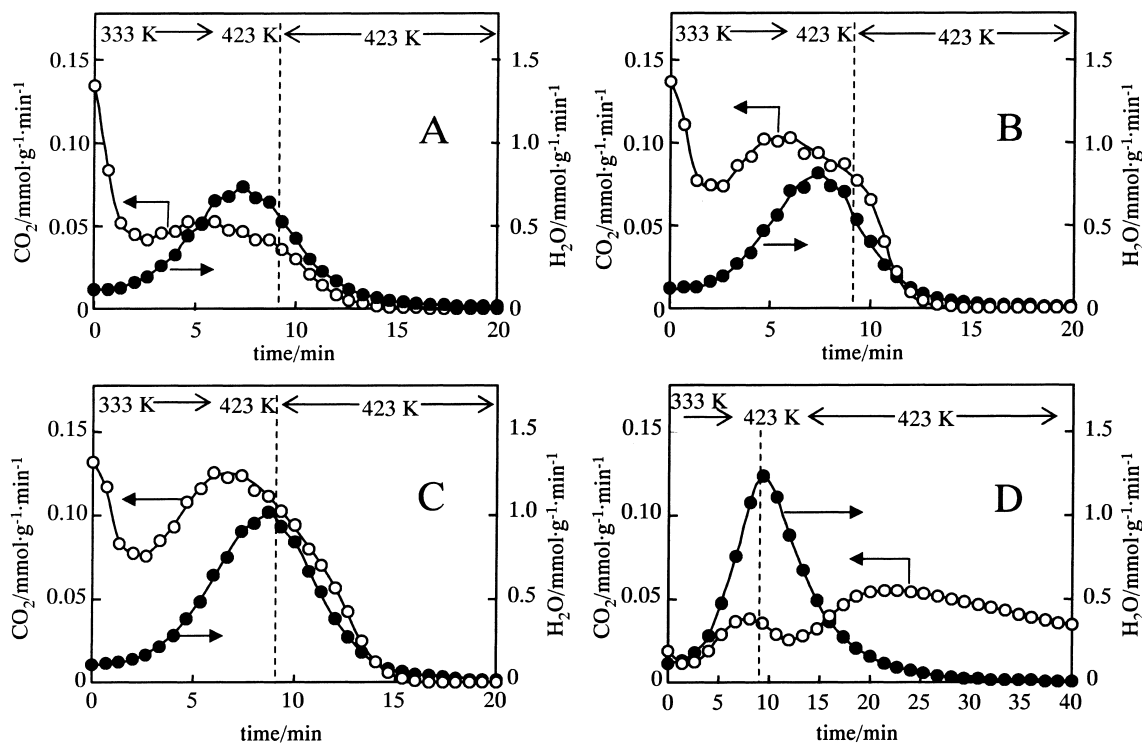
Fig. 6 Desorption of CO_2 (○) and H_2O (●) in a He Flow (30 $cm^3 \cdot min^{-1}$) from APS/SBA (A), AEAPS/SBA (B), TA/SBA (C) and APG (D) after Adsorption (333 K, 15% CO_2, 12% H_2O with N_2 balance)

This result indicates that the amine-CO_2 reaction on APS/SBA, AEAPS/SBA and TA/SBA proceeds immediately, since these amine compounds were anchored and distributed on the surface of the mesoporous support.

The CO_2 and H_2O desorption curves were measured by heating the adsorbents up to 423 K in a He flow after adsorption at 333 K. The desorption curves for APS/SBA, AEAPS/SBA, TA/SBA and APG are shown in **Fig. 6**. The amounts of desorbed CO_2 were consistent with the amounts of adsorbed CO_2, and adsorption capacities were recovered after desorption. The adsorption capacity of APS/SBA at second adsorption (0.49 $mmol \cdot g^{-1}$) was comparable to that at first adsorption (0.50 $mmol \cdot g^{-1}$). Aminosilane-modified SBA-15 was more rapidly regenerated than APG. For example, in the case of TA/SBA (**Fig. 6C**), 77% of adsorbed CO_2 was desorbed before the temperature reached 423 K, and then desorption was completed for 7 min after the temperature reached 423 K. On the other hand, only 9% of adsorbed CO_2 was desorbed from APG before the temperature reached 423 K (**Fig. 6D**), and complete desorption of CO_2 from APG took about 2 h. These results indicate that amine compounds exposed to the surface are optimum for desorption of CO_2.
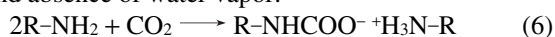
The adsorption state of CO_2 on aminosilane-modified SBA-15 was studied by *in-situ* IR spectroscopy.
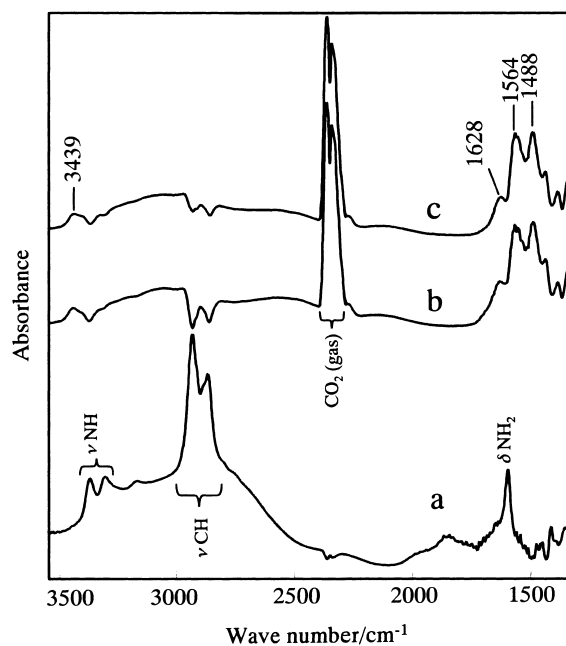
Spectrum b was obtained by subtraction of spectrum a. Spectrum c was obtained by subtraction of the spectrum measured after H_2O adsorption.

Fig. 7 IR Spectrum of Dried APS/SBA (a) and Difference Spectra after CO_2 Adsorption in the Absence (b) and Presence (c) of Water

The IR spectra of surface species formed on APS/SBA by the amine-CO_2 reaction in the presence and absence of water are compared in **Fig. 7**. The IR spectra in the presence and absence of water were identical (spectrum b, c). This result indicates that water does not affect the amine-CO_2 reaction. Absorption bands at 3439 cm^{-1} were attributed to N–H stretch vibration of carbamate (R–NHCOO$^-$, R: alkyl)[16),17)]. Absorption bands at 1628 cm^{-1} and 1563 cm^{-1} and 1488 cm^{-1} were assigned to NH_3^+ deformation, C=O stretch and "NCOO" skeletal vibration of alkylammonium carbamate, respectively[18)]. Therefore, CO_2 is adsorbed on aminosilane-modified SBA-15 through formation of alkylammonium carbamate (Eq. (6)) in the presence and absence of water vapor.

$$2R–NH_2 + CO_2 \longrightarrow R–NHCOO^- {}^+H_3N–R \qquad (6)$$

Carbon dioxide interacts more strongly with aminosilane-modified SBA-15 through formation of alkylammonium carbamate than water vapor which is physically adsorbed on aminosilane-modified SBA-15. The adsorption state of CO_2 on aminosilane-modified SBA-15 is different from that on zeolites, on which both CO_2 and water vapor are adsorbed physically.

4. Conclusion

Novel adsorbents were prepared by modification of SBA-15 with aminosilanes. CO_2 adsorption and desorption proceeded immediately on aminosilane-modified SBA-15, since the amine compounds were uniformly anchored and distributed on the pore walls of the mesoporous support. Furthermore, aminosilane-modified SBA-15 exhibited high adsorption capacities in the presence of water vapor. The results of CO_2 adsorption-desorption experiments demonstrate that these adsorbents are effective for CO_2 separation in the presence of water vapor and are applicable to CO_2 capture and separation from flue gases containing water vapor.

References

1) Ohta, H., Umeda, S., Tajika, M., Nishimura, M., Yamada, M., Yasutake, A., Izumi, J., *Int. J. of Global Energy Issues*, **11**, 203 (1998).
2) Kazama, S., Teramoto, T., Haraya, K., *J. Membr. Sci.*, **207**, 91 (2002).
3) Inui, T., Okugawa, Y., Yasuda, M., *Ind. Eng. Chem. Res.*, **27**, 1103 (1988).
4) Hayashi, H., Taniuchi, J., Furuyashiki, N., Sugiyama, S., Hirano, S., Shigemoto, N., Hirano, S., *Ind. Eng. Chem. Res.*, **37**, 185 (1998).
5) Satyapal, S., Filburn, T., Trela, J., Strange, J., *Energy & Fuels*, **15**, 250 (2001).
6) Leal, O., Bolívar, C., Ovalles, C., García, J. J., Espidel, Y., *Inorg. Chim. Acta*, **240**, 183 (1995).
7) Vansant, E. F., Van Der Voort, P., Vrancken, K. C., *Stud. Surf. Sci. Catal.*, **93**, 193 (1995).
8) Yokoi, T., Tatsumi, T., Yoshitake, H., *J. Colloid Interface Sci.*, **274**, 451 (2004).
9) Han, Y.-J., Stucky, G. D., Butler, A., *J. Am. Chem. Soc.*, **121**, 9897 (1999).
10) Kubota, Y., Nishizaki, Y., Ikeya, H., Saeki, M., Hida, T., Kawazu, S., Yoshida, M., Fujii, H., Sugi, Y., *Microporous Mesoporous Mat.*, **70**, 135 (2004).
11) Chang, A. C. C., Chuang, S. S. C., Gray, M., Soong, Y., *Energy & Fuels*, **17**, 468 (2003).
12) Xu, X., Song, C., Andresen, J. M., Miller, B. G., Scaroni, A. W., *Energy & Fuels*, **16**, 1463 (2002).
13) Xu, X., Song, C., Andresen, J. M., Miller, B. G., Scaroni, A. W., *Microporous Mesoporous Mat.*, **62**, 29 (2003).
14) Zhao, D., Feng, J., Huo, Q., Melosh, N., Fredrickson, G. H., Chmelka, B. F., Stucky, G. D., *Science*, **279**, 548 (1998).
15) Emmett, P. H., Brunauer, S., *J. Am. Chem. Soc.*, **59**, 309 (1938).
16) Battjes, K. P., Barolo, A. M., Dreyfuss, P., *J. Adhes. Sci. Technol.*, **5**, 785 (1991).
17) Eckstein, Y., Dreyfuss, P., *J. Adhesion*, **15**, 163 (1983).
18) Aresta, M., Quaranta, E., *Tetrahedron*, **48**, 1515 (1992).

....

要　　旨

アミノシラン修飾メソポーラスシリカ上への二酸化炭素の吸着

日吉　範人，余語　克則，八嶋　建明

（財）地球環境産業技術研究機構，619-0292 京都府相楽郡木津町木津川台9-2

メソポーラスシリカ SBA-15 に種々のアミノシランをグラフトすることによりアミノシラン修飾メソポーラスシリカを調製し，排ガスからの CO_2 分離回収用新規吸着剤としての適用可能性を検討した。グラフト法により SBA-15 の細孔壁はアミノシランで均一に修飾され，比較的大きな表面積と均一な細孔径が保たれた。流通法により水蒸気共存条件での CO_2 吸着量を水蒸気非共存条件での CO_2 吸着量と比較した。アミノシラン修飾 SBA-15 の吸着量は水蒸気が共存しても水蒸気が共存しない場合と同等であることが分かった。特に，（3-トリメトキシシリルプロピル）ジエチレントリアミンを固定化した SBA-15 の CO_2 吸着量は水蒸気共存条件においても 333 K で 1.2 mol・kg^{-1} に達し，水蒸気が存在しない場合のゼオライト Na-Y の CO_2 吸着量と同等であった。また，二酸化炭素を吸着したアミン修飾 SBA-15 は，He 気流中 423 K まで加熱することにより完全に再生された。

....